Molecular Crystals and Liquid Crystals
Publication details, including instructions for authors and subscription information:
http://www.tandfonline.com/loi/gmcl20

Thermal Degradation and Combustion Behavior of Polypropylene/MWCNT Composites

G. E. Zaikov [a], A. D. Rakhimkulov [a], S. M. Lomakin [a], I. L. Dubnikova [b], A. N. Shchegolikhin [a], E. Ya. Davidov [a] & R. Kozlowski [c]

[a] NM Emanuel Institute of Biochemical Physics of Russian Academy of Sciences, Moscow, Russia

[b] NN Semenov Institute of Chemical Physics of Russian Academy of Sciences, Moscow, Russia

[c] Institute of Natural Fibres, Poznan, Poland

To cite this article: G. E. Zaikov, A. D. Rakhimkulov, S. M. Lomakin, I. L. Dubnikova, A. N. Shchegolikhin, E. Ya. Davidov & R. Kozlowski (2010): Thermal Degradation and Combustion Behavior of Polypropylene/MWCNT Composites, Molecular Crystals and Liquid Crystals, 523:1, 106/[678]-119/[691]

To link to this article: http://dx.doi.org/10.1080/15421401003726543

Mol. Cryst. Liq. Cryst., Vol. 523: pp. 106/[678]–119/[691], 2010
Copyright © Taylor & Francis Group, LLC
ISSN: 1542-1406 print/1563-5287 online
DOI: 10.1080/15421401003726543

Thermal Degradation and Combustion Behavior of Polypropylene/MWCNT Composites

G. E. ZAIKOV,[1] A. D. RAKHIMKULOV,[1]
S. M. LOMAKIN,[1] I. L. DUBNIKOVA,[2]
A. N. SHCHEGOLIKHIN,[1] E. YA. DAVIDOV,[1] AND
R. KOZLOWSKI[3]

[1]NM Emanuel Institute of Biochemical Physics of Russian Academy of Sciences, Moscow, Russia
[2]NN Semenov Institute of Chemical Physics of Russian Academy of Sciences, Moscow, Russia
[3]Institute of Natural Fibres, Poznan, Poland

Studies of thermal and fire-resistant properties of the polypropylene/multi-walled carbon nanotube composites (PP/MWCNT) prepared by means of melt intercalation are discussed. The sets of the data acquired with the aid of non-isothermal TG experiments have been treated by the model kinetic analysis. The thermal-oxidative degradation behavior of PP/MWCNT and stabilizing effect caused by addition of MWCNT has been investigated by means of TGA and EPR spectroscopy. The results of cone calorimetric tests lead to the conclusion that char formation plays a key role in the mechanism of flame retardation for nanocomposites. This could be explained by the specific antioxidant properties and high thermal conductivity of MWCNT which determine high-performance carbonization during thermal degradation process. Comparative analysis of the flammability characteristics for PP-clay/MWCNT nanocomposites was provided in order to emphasize the specific behavior of the nanocomposites under high-temperature tests.

Keywords Antioxidants; carbon nanotubes; combustion; composites; cone calorimetric test; ESR spectroscopy; kinetic analysis; melt intercalation; multi-walled; polypropylene; TG; TGA; thermal conductivity; thermal degradation

Introduction

At present time the great attention is given to the study of properties of polymeric nanocomposites produced on the basis of well-known thermoplastics (PP, PE, PS, PMMA, polycarbonates, polyamides) and carbon nanotubes (CN). CNs are considered to have the wide set of important properties like thermal stability, reduced combustibility, electroconductivity, etc. [1–7]. Thermoplastic polymer nanocomposites are generally produced with the use of melting technique [1–12].

Address correspondence to G. E. Zaikov, NM Emanuel Institute of Biochemical Physics, Russian Academy of Sciences, 4 Kosygin Str., Moscow 119334, Russia. Tel.: +7-495-939-7191; Fax: +7-499-137-4101; E-mail: Chembio@sky.chph.ras.ru

Development of synthetic methods and the thermal characteristics study of PP/multi-walled carbon nanotube (MWCNT) nanocomposites were taken as an objective in this paper.

A number of papers pointed at synthesis and research of thermal properties of nanocomposites (atactic polypropylene (aPP)/MWCNT) were reported [10–12]. It is remarkable that PP/MWCNT composites with minor level of nanocarbon content (1–5% by weight) were determined to obtain an increase in thermal and thermal-oxidative stability in the majority of these publications.

Thermal stability of aPP and aPP/MWCNT nanocomposites with the various concentrations of MWCNT was studied in the paper [10]. It was shown that thermal degradation processes are similar for aPP and aPP/MWCNT nanocomposites and initial degradation temperatures are the same. However, the maximum mass loss rate temperature of PP/MWCNT nanocomposites with 1 and 5% wt of MWCNT raised by 40–70°C as compared with pristine aPP.

Kashiwagi *et al.* published the results of study of thermal and combustion properties of PP/MWCNT nanocomposites [11,12]. A significant decrease of maximum heat release rate was detected during combustion research with use of cone calorimeter. A formation of char network structure during the combustion process was considered to be the main reason of combustibility decrease. The carbonization influence upon combustibility of polymeric nanocomposites was widely presented in literature [10–12,13]. Notably, Kashiwagi *et al.* [11,12] were the first to hypothesize that abnormal dependence of maximum heat release rate upon MWCNT concentration is closely related with thermal conductivity growth of PP/MWCNT nanocomposites during high-temperature pyrolysis and combustion.

Experimental

Materials

Isotactic polypropylene (melting flow index = 0.7 g/10 min) was used as a polymer matrix in this paper. Multi-walled carbon nanotubes (MWCNT) (purchased from Shenzhen Nanotechnologies Co. Ltd.) were used as a carbon-containing nanofillers. This product contains low amount of amorphous carbon (less than 0.3 wt%) and could be produced with different size characteristics-different length and different diameter and therefore different diameter to length ratio. Size characteristics for three MWCNT used in this paper are given in Table 1. Sizes and structure of initial MWCNT were additionally estimated by SEM (Fig. 1).

Table 1. Properties of MWCNT

Designation	D, nm	L, μm	Density, g/cm^3	Specific surface area, m^2/g
MWCNT (К1)	<10	5–15	2	40–300
MWCNT (К2)	40–60	1–2	2	40–300
MWCNT (К3)	40–60	5–15	2	40–300

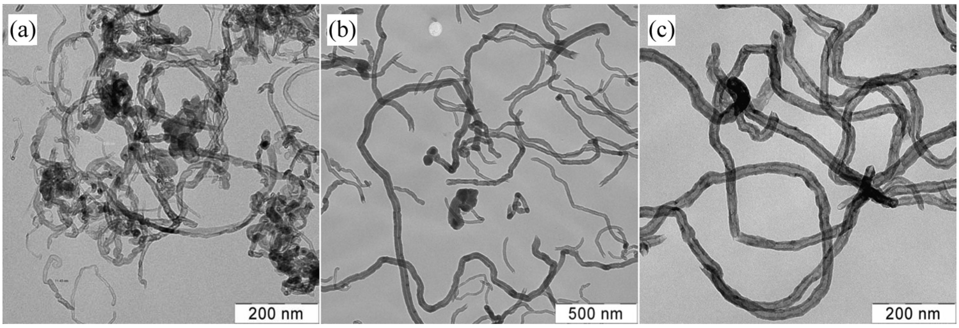

Figure 1. SEM images of original MWCNTs: (a) MWCNT(1); (b) MWCNT(2); (c) MWCNT(3).

Nanocomposite Processing

Compositions were prepared by blending carbon nanotubes with melted polymer in a laboratory mixer Brabender at 190°C. TOPANOL® (1,1,3-tris(2-methyl-4-hydroxy-5-t-butylphenyl)butane) and DLTP (dilaurylthiodipropionate) were added in the amount of 0.3 and 0.5 wt% as antioxidants to prevent thermal-oxidative degradation during polymer processing.

A number of different covalent and non-covalent nanotube modifications (organofillization) were reported to be used to achieve greater structure similarity and therefore greater nanotube distribution in a polymer matrix [14–20]. In order to functionalize MWCNT we used preliminary ozone treatment of MWCNT followed by ammonolysis of epoxy groups on the MWCNT surface. The selective ozonization of MWCNT was carried out with ozone-oxygen mixture (ozone concentration was 2.3×10^{-4} mol/L) in a bubble reactor. Then the ammonolysis of oxidized MWCNT has been carried out by *tert*-butylamine in the ultrasonic bath (35 kHz) at 50°C for 120 min with following evaporation of *tert*-butylamine excess. IR transmission spectra of tablet specimens of MWCNTs in KBr matrix was analyzed by using Perkin-Elmer 1725X FTIR spectrometer and the presence of the alkylamine groups at the MWCNT surface was confirmed by the appearance of the characteristic band $\sim 1210\,\text{cm}^{-1}$ corresponding to the valency vibration of the bond $-\text{C}-\text{N}\leftarrow$.

Investigation Techniques

Scanning Electron Microscopy (SEM). The degree of MWCNT distribution in polymer matrix was analyzed with scanning electron microscope JSM-35. Low-temperature chips derived from film-type samples were used for this analysis.

Transmission Electron Microscopy (TEM). The degree of nanotube dispersion in polymer matrix was studied with transmission electron microscopy (LEO912 AB OMEGA, Germany). Microscopic sections with 70–100 nm width prepared with ultramicrotome "Reichert–Jung Ultracut" with diamond cutter at −80°C. Microscopic analysis was made with accelerating potential of about 100 kV without chemical sample staining.

Thermogravimetric Analysis (TG). A NETZSCH TG 209 F1 Iris thermomicrobalance has been employed for TGA measurements in oxidizing (oxygen) atmosphere. The measurements were carried out at a heating rate of 20 K/min.

Combustibility Characteristics (Cone Calorimeter). Were performed according to the standard procedures ASME E1354/ISO 5660 using a DUAL CONE 2000 cone-calorimeter (FTT). An external radiant heat flux of 35 kW/m^2 was applied. All of the samples having a standard surface area of 70 × 70 mm and identical masses of 13.0 ± 0.2 g were measured in the horizontal position and wrapped with thin aluminum foil except for the irradiated sample surface.

Heat Capacity and Heat Conductivity. Heat capacity and heat conductivity were determined with the use of NETZSCH 457 *MicroFlash*.

The electron paramagnetic resonance spectroscopy (EPR) measurements were performed in air with the PP/MWCNT (10 wt%) samples using a Mini-EPR SPIn Co. Ltd spectrometer with 100 kHz field modulation. The *g* factor and EPR intensity (X-band) were measured with respect to a standard calibrating sample of Mn^{2+} and ultramarine.

Results and Discussion

Nanocomposite Structure

Dispersion analysis of MWNT in nanocomposites. PP/MWNT nanocomposites with original and modified MWNT were produced. Filler concentration varied from 1 to 7 wt% weight percent (0.5–3.5 volume percent correspondingly). Distribution pattern for composites with modified and non-modified nanotubes was studied with TEM methods (Fig. 2). According to TEM images the addition of 1% by weight leads to sufficiently uniform distribution. However, agglomeration of nanotubes was detected for more concentrated nanocomposites, especially for PP/MWNT with MWNT average diameter less than 10 nm (K1).

TEM images for PP nanocomposites with 5 wt% modified and non-modified MWNT (2.5% by volume) are shown on Figure 2. According to Figure 2 it could be stated that modified nanotubes (K2 and K3) used during melding process are present as individual particles in nanocomposite in most cases. The number and size of agglomerates is reduced due to increased organophility and improved thermodynamic compatibility with nonpolar polymer.

However, preliminary modification doesn't not lead to uniform filler distribution for nanocomposites containing thin nanotubes (K1). This could be explained by the

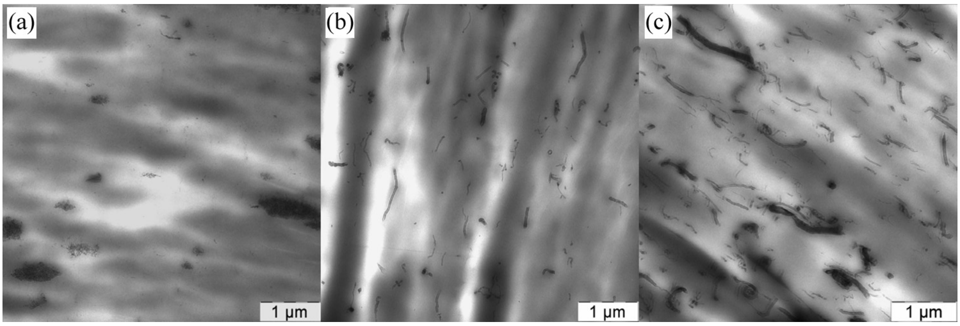

Figure 2. TEM images of PP/MWCNT nanocomposites showing dispersion of MWCNT in a polymer matrix: (a) PP/MWCNT(1); (b) PP/MWCNT(2); (c) PP/MWCNT(3).

fact that interaction energy of CNT is more dependent on nanotube diameter than of its length. Molecular dynamic computation given in paper [24] showed that blending polymers with nanotubes becomes more thermodynamically favorable with increase of nanotubes diameter, owing to the fact that cohesion energy is decreased between the nanotubes and remains almost the same between nanotubes and polymer.

Thus, mixing the thinnest nanotubes (K1) with PP leads to inevitable nanotube agglomeration in nanocomposite sample volume. Nanotube surface modification used in this paper didn't result in complete overcome of nanotube agglomeration tendency for K1 nanotubes [25]. Therefore, the PP/MWNT(K3) nanocomposites presented the main subjects of inquiry in the present study.

Thermal-Oxidative Degradation of PP/MWCNT Nanocomposites

The diverse behavior of PP and PP/MWCNT nanocomposites with 1, 3 and 5 wt% of MWCNT(3). Figure 3 shows that the influence of MWCNTs on the thermal-oxidation process resulted in higher thermal-oxidative stability of PP/MWCNT nanocomposites. It is possible to see a regular increase in the temperature values of the maximum mass loss rates (up to 60°C) for the PP/MWCNT as compared to pristine PP (Fig. 3).

Detailed analysis of TGA graphs (Fig. 3) allows claiming that thermal stability increase is achieved even by addition of 1 wt% of MWCNT to PP, while further addition doesn't lead to such fundamental growth. In addition, Figure 4 shows the comparative results for onset degradation temperatures ($T_{on.}$) and the maximum mass loss temperatures (T_{max}) of PP/MWCNT nanocomposites with the different

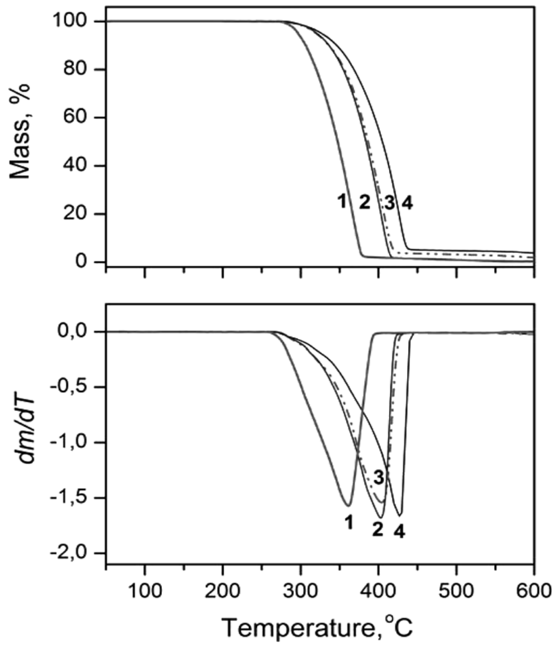

Figure 3. TG and DTG curves for PP (1) and PP/MWCNT(3) composites with 1 (2), 3 (3) and 5 wt% (4) filler loadings.

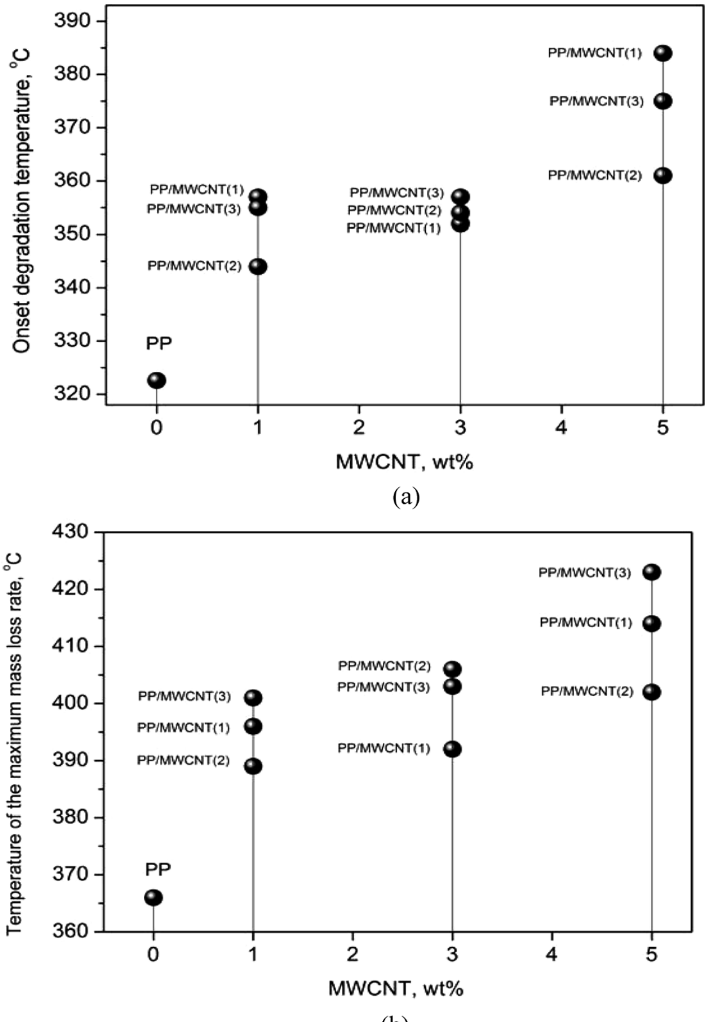

Figure 4. Comparative diagrams showing the onset degradation temperatures (a) and the maximum mass loss temperatures (b) for PP and PP/MWCNT nanocomposites with the different types and concentrations of MWCNT.

types and concentrations of MWCNT. One can see nonlinear relation of ($T_{on.}$) and (T_{max}) vs. MWCNT concentration in the PP compositions (Fig. 4).

At the present time the nature of thermal stability effect caused by MWCNT addition to polymers is an object of comprehensive study. Most likely, MWCNTs could be considered as high temperature stabilizers (antioxidants) in reactions of thermal-oxidative degradation by analogy with fullerenes [6]. Stabilizing effect caused by addition of MWCNT was previously detected for PP/MWCNT nanocomposites [8]: the temperature of the maximum mass loss rates of PP/MWCNT (9 wt%) was increased by 50°C as compared with pristine PP.

Results achieved in this study confirm the previous findings of the inhibiting effect of MWNCT upon the PP/MWCNT nanocomposite thermal-oxidative degradation. Obviously, the complex nature of this effect is closely related to radical-acceptor properties of MWCNT resulting in chain termination reactions of alkyl/alkoxyl radical, which lead to cross-linking and carbonization process in PP/MWCNT nanocomposites. Carbonization phenomenon was reported previously in papers aimed at PP/MWCNT heat resistance and flame retardancy study [11,12].

Kinetic Analysis of Thermal Degradation of PP/MWNT

Kinetic studies of material degradation have long history, and there exists a long list of data analysis techniques employed for the purpose. Often, TGA is the method of choice for acquiring experimental data for subsequent kinetic calculations, and namely this technique was employed here. It is commonly accepted that the degradation of materials follows the base Eq. (1) [7]

$$dc/dt = -F(t, T, c, p) \tag{1}$$

where: t-time, T-temperature, c_o-initial concentration of the reactant, and p-concentration of the final product. The right-hand part of the equation $F(t, T, c, p)$ can be represented by the two separable functions, $k(T)$ and $f(c, p)$:

$$F(t, T, c, p) = k[T(t) \cdot f(c, p)] \tag{2}$$

Arrhenius Eq. (4) will be assumed to be valid for the following:

$$k(T) = A \cdot \exp(-E/RT) \tag{3}$$

Therefore,

$$dc/dt = -A \cdot \exp(-E/RT) \cdot f(c, p) \tag{4}$$

All feasible reactions can be subdivided onto classic homogeneous reactions and typical solid-state reactions, which are listed in Table 2. The analytical output must provide good fit to measurements with different temperature profiles by means of a common kinetic model.

Thermogravimetric analysis of PP and PP nanocomposite degradation was carried out in dynamic conditions at the rates of 2.5, 5 and 10 K/min on air. Model-independent estimation of activation energy using Friedman approach [28] was taken to get preliminary model analysis for thermal degradation and selection of initial conditions. According to this evaluation, a two-step process ($A \rightarrow X_1 \rightarrow B \rightarrow X_2 \rightarrow C$) was chosen for PP degradation. Taking into account the carbonization stage the more complex three-step process ($A \rightarrow X_1 \rightarrow B \rightarrow X_2 \rightarrow C \rightarrow X_3 \rightarrow D$) was selected for PP/MWNT degradation [7,9].

According to the results of nonlinear regression and taking the set of reaction models into consideration we computed the values of active kinetic parameters, which represent the best approximation of experimental TGA graphs (Fig. 5, Table 3).

Two-step PP thermal-oxidative degradation in dynamic heating conditions was confirmed by obtained data [20]. At the first stage the values of activation energy and pre-exponential factor are 110.25 kJ/mol and $10^{9.5}\,s^{-1}$ correspondingly, while the

Table 2. Considered reaction models $dc/dt = -A \cdot exp(-E/RT)f(c, p)$

Reaction models	$f(c, p)$
First order (F_1)	c
Second order (F_2)	c^2
n-order (F_n)	c^n
Two-dimensional phase boundary (R_2)	$2 \cdot c^{1/2}$
Three-dimensional phase boundary (R_3)	$3 \cdot c^{2/3}$
One-dimensional diffusion (D_1)	$0.5/(1-c)$
Two-dimensional diffusion (D_2)	$-1/ln(c)$
Three-dimensional diffusion, Jander's type (D_3)	$1.5c^{1/3}(c^{-1/3}-1)$
Three-dimensional diffusion, Ginstling-Brounstein (D_4)	$1.5/(c^{-1/3}-1)$
One-dimensional diffusion (Fick law) (D_{1F})	–
Three-dimensional diffusion (Fick law) (D_{3F})	–
Prout-Tompkins equation (B_1)	$c \cdot p$
Expanded Prout-Tompkins equation (B_{na})	$c^n \cdot p^a$
First order reaction with autocatalysis by X ($C_{1\text{-}X}$)	$c \cdot (1 + K_{cat}\ X)$
n-order reaction with autocatalysis by X ($C_{n\text{-}X}$)	$c^n \cdot (1 + K_{cat}\ X)$
Two-dimensional nucleation, Avrami-Erofeev equation (A_2)	$2 \cdot c \cdot (-ln(c))^{1/2}$
Three-dimensional nucleation, Avrami-Erofeev equation (A_3)	$3 \cdot c \cdot (-ln(c))^{2/3}$
n-dimensional nucleation, Avrami-Erofeev equation (A_n)	$n \cdot c \cdot (-ln(c))^{(n-1)/n}$

reaction order is close to 2 (1.89). The values of activation energy and pre-exponential factor are larger on the second stage ($E_2 = 150.65$ kJ/mol, $A_2 = 10^{15.3}\ s^{-1}$) with effective reaction order of $n_2 = 1.50$.

The preferred model for PP/MWNT thermal-oxidative degradation and with respect to statistical analysis of kinetic parameters is composed of 3 consecutive reactions $F_n \rightarrow D_1 \rightarrow F_n$, where D_1 – one-dimensional diffusion, and F_n – n-order reaction (Fig. 4b, Table 3b). In this case the first step activation energy is equal to 105.1 kJ/mol, reaction order is close to 1 ($n_1 = 0.91$). On the second step, which is described as one-dimensional diffusion, the value of activation energy is equal 120.4 kJ/mol, while the value is almost twice large for the third step ($E_3 = 229.5$ kJ/mol) with effective reaction order of $n_3 = 0.5$ (Table 3b).

Comparison of thermal oxidative degradation parameters for PP/MWNT with layered silicate PP//MMT showed that the values of activation energy of the second and the third stages are higher for PP/MWNT:

$E_2 = 120.4$ kJ/mol and $E_3 = 229.5$ kJ/mol for PP/MWNT;
$E_2 = 100.0$ kJ/mol and $E_3 = 199.8$ kJ/mol for PP/MPP/MMT correspondingly [20].

This data may testify to more intensive carbonization in case of PP/MWNT than in case of PP/MMT, which finally leads to decrease in RHR value.

Combustibility of PP/MWCNT Nanocomposites

Figure 6 depicts the plots of the heat release rate (RHR), as basic flammability characteristic, vs. time for PP, as well as for the PP/MWCNT nanocomposites.

From Figure 6, it could be seen that the maximum heat release rate for pristine PP is 2076 kW/m^2, whereas that for the PP/MWCNT % nanocomposites (1 wt%),

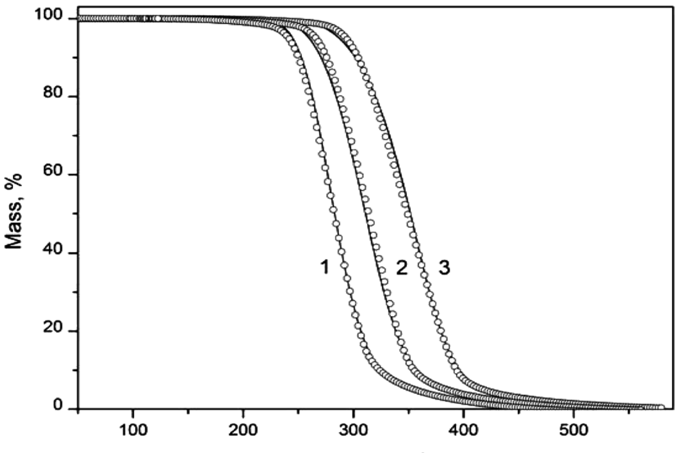

(a)

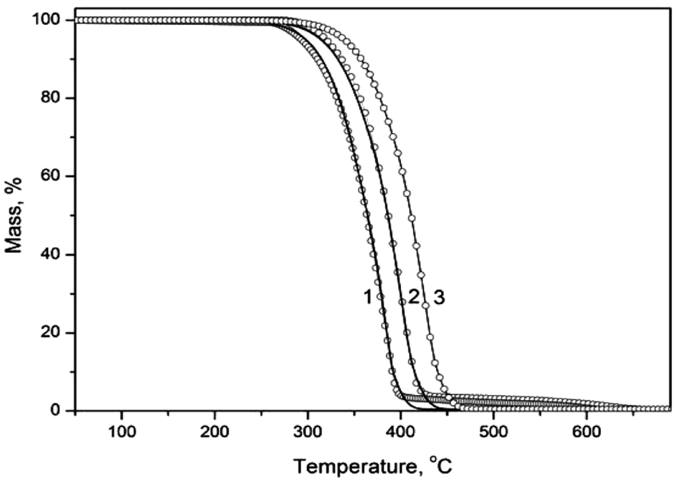

(b)

Figure 5. Nonlinear kinetic modeling of a – PP and b – PP/MWCNT(3) thermal-oxidative degradation in air. Comparison between experimental TG data (dots) and the model results (firm lines) at several heating rates: (1) −2.5, (2) −5, (3) −10 K/min.

PP/MCWNT (3 wt%) and the PP/MCWNT (5 wt %) RHR values are 729 kW/m^2, 552.8 kW/m^2, and 455.8 kW/m^2, respectively; thus, the peak heat release rate decreases by 65%, 73% and 78%.

The observed flame retardancy effect is associated with solid-phase carbonization reactions, by analogy with layered silicates [11,12]. In early paper [20] we have found that additions of 3 and 7 wt % of layered silicate (Cloisite 20A) to the PP compositions PP lead to RHR decrease by 51 and 57% as compared with pristine PP (Fig. 5).

We believe that a higher carbonization effectiveness of MWCNTs depends on their heat conductivity. It is well known that, PP has a low thermal conductivity at standard conditions, and characterized by a minor increase with temperature

Table 3. Kinetic parameters for thermal degradation of (a) PP (**Fn → Fn**) and (b) PP/MWNT nanocomposite (**Fn → D1 → Fn**). TGA analysis was performed in air flow with the use of multiple non-linear regression analysis for model processes

Reaction model	Kinetic parameters	Values	Correlation coefficient
(a) Fn → Fn	$\log A_1$, s^{-1}	9.53	0.9996
	E_1, kJ/mol	110.25	
	n_1	1.89	
	$\log A_2$, s^{-1}	15.25	
	E_2, kJ/mol	150.65	
	n_2	1.50	
(b) Fn → D1 → Fn	$\log A_1$, s^{-1}	6.3	0.9996
	E_1, kJ/mol	105.1	
	n_1	0.91	
	$\log A_2$, s^{-1}	7.4	
	E_2, kJ/mol	120.4	
	$\log A_3$, s^{-1}	16.7	
	E_3, kJ/mol	229.5	
	n_3	0.5	

up to melting point (~0.2 W/m K). On the other hand the heat conductivity of individual MWCNT is extremely high and equals to 3000 W/m K [13,14]. During the high temperature pyrolysis of PP/MWCNT composition at temperatures above 300–400°C the heat conductivity can rise up to 20 W/m K [14] due to actual increase of MWCNT concentration in composition caused by volatilization of polypropylene degradation products (Fig. 7). The induced heating of PP/MWCNT intensifies a

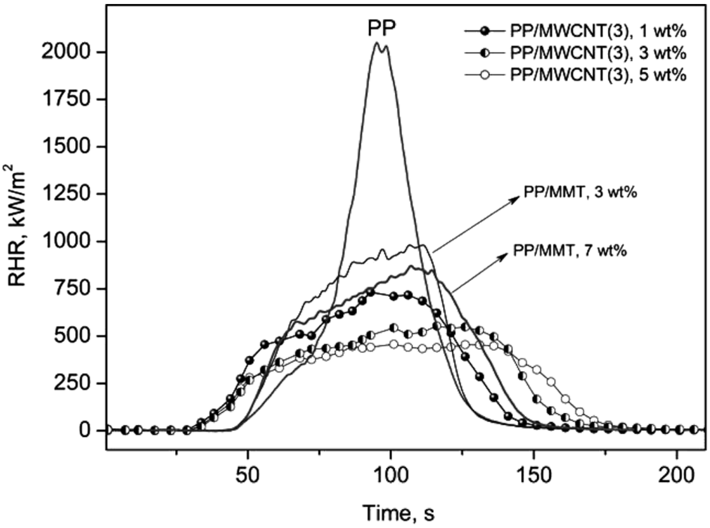

Figure 6. Rate of heat release vs. time for PP, PP/MWCNT and PP/MMT (Cloisite 20A) nanocomposites obtained by cone calorimeter at the incident heat flux of 35 kW m^{-2}.

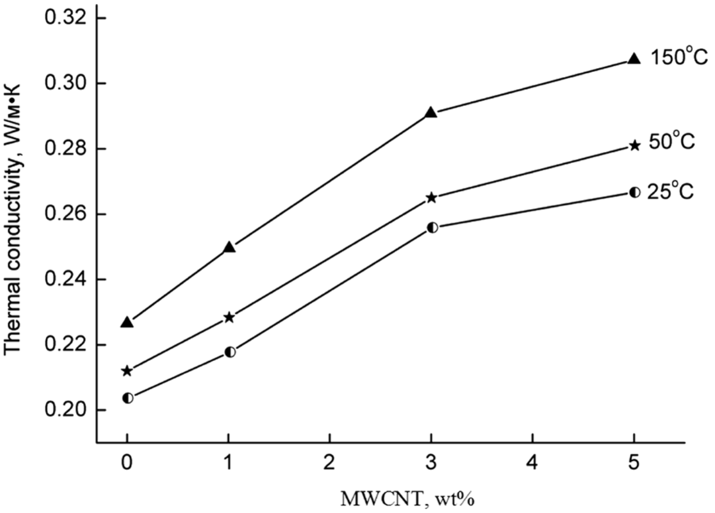

Figure 7. Temperature dependence of the thermal conductivity of PP/MWCNT (3) nanocomposite with different loadings of MWCNT.

steady carbonization and charring of the samples and leads to decrease of RHR peak value (Fig. 6).

Figures 8 and 9 show graphs for the specific extinction area and effective heat of combustion, correspondingly, for PP and PP/MWCNT(3) nanocomposites. Calculated values of effective heat of combustion for PP and PP/MWNT demonstrate invariant shift of this parameter for these nanocomposites.

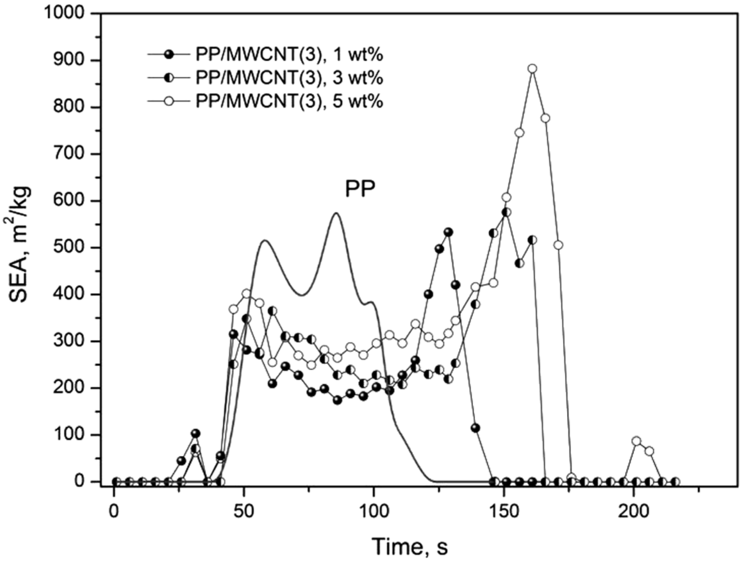

Figure 8. Specific extinction area vs. time for PP and PP/MWCNT(3) nanocomposites obtained by cone calorimeter at the incident heat flux of 35 kW m^{-2}.

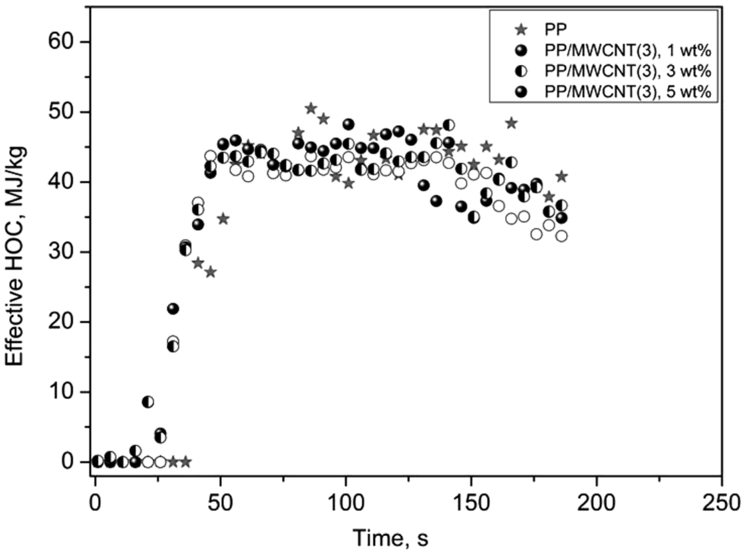

Figure 9. Effective heat of combustion vs. time for PP and PP/MWCNT(3) nanocomposites obtained by cone calorimeter at the incident heat flux of 35 kW m^{-2}.

In the present study EPR research were performed to follow formation of stable radicals, responsible for carbonization process, upon isothermal heating of PP/MCWNT (10 wt%) in air at 350°C.

Figure 10a shows EPR spectrum of the stable paramagnetic centers formed in the samples of PP/MCWNT (10% wt) heating in air at 350°C. When a heated in air PP/MCWNT specimen was placed into an EPR sample tube, a narrow singlet signal with a line width of $\Delta H_{1/2} = 0{,}69\,\text{mT}$ and a g value of 2.003 was detected due to the stable radicals generation, analogous to those previously registered during polymers carbonization process [15]. No EPR signal similar to that of PP/MCWNT

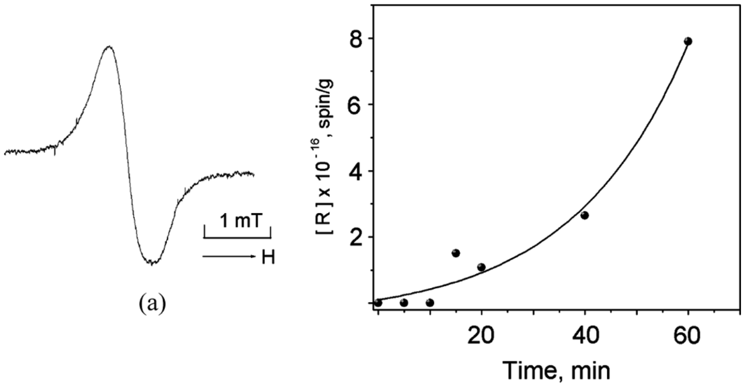

(a)

(b)

Figure 10. EPR spectrum of the stable paramagnetic centers formed in the samples of PP/MCWNT (10% wt) heating in air at 350°C – (a), kinetic dependence of stable radicals generation from PP/MCWNT (10% wt) under isothermal heating at 350°C in air – (b).

samples were observed in the samples of pristine PP and MCWNT samples heated at 350°C in air. It should be noted that although iron impurity from MWNCT has been mentioned in other studies on pyrolysis of polymer nanocomposites as the radical traps [11,16], the EPR analyses in the current study showed the presence of paramagnetic centers relating to carbonaceous stable radicals only.

As it is seen from Figure 10b, the formation of stabilized radicals occurs with pronounced induction period which is related to antioxidant properties of MWNCT. Such a type of kinetic dependence is coincided with an oxygen uptake kinetics observed during inhibited polyolefines thermal oxidation. Moreover, no EPR signals were observed in the samples of the PP/MCWNT samples heated at 350°C in inert Ar.

Thus, multi-walled carbon nanotubes are considered to be more effective filling agents than layered silicates in the terms of improvement of thermal properties and flame retardancy of PP matrix. This could be explained by the specific antioxidant properties and high thermal conductivity of MWCNT, which determine the carbonization reactions during thermal-oxidative degradation process.

References

[1] Lomakin, S. M., Dubnikova, I. L., Zaikov, G. E., Kozlowski, R. M., Kim, G. M., & Michler, G. H. (2009). *Rubber, Fibres, Plastics International Journal*, *4*, 181.

[2] Khalturinskii, N. A., Novikov, D. D., Zhorina, L. A., Kompaniets, L. V., Rudakova, T. A., & Barbot'ko, S. L. (2009). *All Materials Journal (Russian)*, *4*, 8.

[3] Aseeva, R. M. & Zaikov, G. M. (1981). *Combustion of Polymer Materials*, Nauka Publishers: Moscow, USSR.

[4] Aseeva, R. M. & Zaikov, G. M. (1981). *Decreasing of Flammability of Polymer Materials*, Znanie Publishers: Moscow, USSR.

[5] Aseeva, R. M. & Zaikov, G. M. (1986). *Combustion of Polymer Materials*, Karl Hanser Verlag: Munchen, FRG.

[6] Lomakin, S. M. & Zaikov, G. E. (1999). *Ecological Aspects of Polymer Flame Retardancy*, VSP International Science Publishers: Utrecht, The Netherlands.

[7] Zaikov, G. E. & Khalturinskii, N. A. (2000). *Low Flammability of Polymeric Materials*, Nova Science Publishers: New York, USA.

[8] Buchachenko, A. L., Zaikov, G. E., & Ivanov, V. B. (2002). *Aging of Polymers, Polymer Blends and Polymer Composites*, Nova Science Publishers: New York, USA, Vol. 1.

[9] Buchachenko, A. L., Zaikov, G. E., & Ivanov, V. B. (2002). *Aging of Polymers, Polymer Blends and Polymer Composites*, Nova Science Publishers: New York, USA, Vol. 2.

[10] Buchachenko, A. L., Zaikov, G. E., & Ivanov, V. B. (2002). *Polymer Aging at the Cutting Edge*, Nova Science Publishers: New York, USA.

[11] Lomakin, S. M. & Zaikov, G. E. (2003). *Polymer Flame Retardancy*, VSP International Science Publishers: Utrecht, The Netherlands.

[12] Lomakin, S. M., Zaikov, G. E., & Koverzanova, E. V. (2005). Fire retardancy of polymers. In: *The Thermal Degradation and Combustion of Polypropylene Filled with Magnesium Hydroxides Micro-Fillers and Polypropylene Nano-Filled Alumo Silicate Composites*, Le Bras, M., Wilkie, Ch. A., Bourbigot, S., Duquesne, S., & Jama, Ch. (Eds.), The Royal Chemical Society: Cambridge, UK, Chapter 7, 100–113.

[13] Zaikov, G. E., Lomakin, S. M., & Sheptalin, R. A. (2005). Fire retardancy of polymers. In: *Pyrolysis and Flammability of Polyurethane-Organophilic Clay Nanocomposite*, Le Bras, M., Wilkie, Ch. A., Bourbigot, S., Duquesne, S., & Jama, Ch. (Eds.), The Royal Chemical Society: Cambridge, UK, Chapter 10, 139–146.

[14] Zaikov, G. E., Lomakin, S. M., & Sheptalin, R. A. (2005). Fire retardancy of polymers. In: *Comparison of the Degradation Products of Polyurethane and Polyurethane-Organophilic Clay Nanocomposite. Toxicological Aspects*, Le Bras, M., Wilkie, Ch. A., Bourbigot, S., Duquesne, S., & Jama, Ch. (Eds.), The Royal Chemical Society: Cambridge, UK, Chapter 27, 363–371.

[15] Kozlov, G. V., Yanovskii, Yu. G., & Karnet, Yu. N. (2008). *Structure and Properties of Filled Polymer Composites and Nanocomposites*, Al'yanstransatom Publishers: Moscow, Russia.

[16] Kozlov, G. V. & Zaikov, G. E. (2009). *Claster Model Interaction with Modern Physical Concepts*, Nova Science Publishers: New York, USA.

[17] Pethrick, R. A., Zaikov, G. E., & Pielichowski, J. (2009). *Progress in Monomers, Oligomers, Polymers, Composites and Nanocomposites*, Nova Science Publishers: New York, USA.

[18] Thomas, S. & Zaikov, G. E. (2008). *Progress in Polymer Nanocomposite Research*, Nova Science Publishers: New York, USA.

[19] Thomas, S., Zaikov, G. E., & Valsaraj, S. V. (2009). *Present Advances in Polymer Nanocomposites*, Brill Academic Publishers: Boston-Leiden, The Netherlands.

[20] Zaikov, G. E. (2009). *Polymer Material Science. New Horizons, Nauchnye Osnovy i Tekhnologii*, (Scientific foundation and technologies) Publishers: St. Petersburg, Russia.